

Mechanism of Cis/Trans Equilibration of Alkenes via Iodine Catalysis

Steven S. Hepperle, Qingbin Li, and Allan L. L. East*

Department of Chemistry and Biochemistry, University of Regina, Regina, Saskatchewan, S4S 0A2 Canada

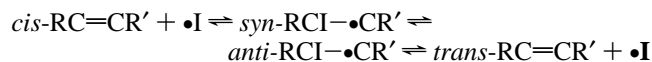
Received: July 7, 2005; In Final Form: September 30, 2005

Iodine is commonly used to speed the equilibration of Wittig cis/trans alkene products. This study uses computational chemistry to study the catalyzed isomerization mechanism in detail for seven different examples of 1,2-disubstituted alkenes. We find that the iodo intermediates of the conventional three-step reaction path are weakly stable, bound by less than 7 kJ mol⁻¹ in five cases and nonexistent in the other two. These variations in relative stability appear to be closely related to the degree of conjugation interruption in the alkene upon attachment of iodine. The rate-determining reaction barrier always occurs in the middle step, the internal rotation of the iodo intermediate, and the variations in the barrier heights are dictated by varying levels of steric hindrance in the seven cases. Regiospecificity of I-atom addition and noticeable hyperconjugative effects are discussed. Comparisons between various theoretical approximations are performed to demonstrate the great difficulty in obtaining accurate results for iodine-atom bond-forming and bond-breaking energies.

Introduction

The ability of iodine to speed the equilibration of alkenes has been known since the 19th century.¹ In the 1960s, Benson and co-workers exploited this reaction in the gas phase to obtain accurate relative energies of alkenes;² their initial work on butene revealed both positional (hydrogen-shift)^{3–6} and geometrical (cis/trans)^{3–5,7} isomerism. Back and Cvetanovic investigated the gas-phase butene reactions as well, at milder temperatures.^{8,9} In solution, both of these forms of isomerization were also observed, in an Oxford study of *cis*-4-octene catalyzed by iodine.¹⁰ Since the 1960s, iodine catalysis to convert *cis*-alkenes to *trans* forms has become a routine tool in organic synthesis, e.g., for purifying Wittig-reaction products, which can be *cis/trans* mixtures;^{11,12} we cite, for example, the use of iodine in the preparations of parent¹³ and substituted^{14,15} stilbene (1,2-diphenylethene).

The assumed mechanism for *cis/trans* isomerism, suggested in the 1930s on the basis of kinetics studies¹ and adopted by Benson,⁷ is a three-step process involving attachment of an iodine atom, an internal rotation, and a detachment of the iodine atom



Iodine atoms are easily formed from I₂ either thermally or photolytically. The more complicated mechanism of Back and Cvetanovic,⁸ involving three types of intermediates (freely rotating RCI-•CR', π complexes of •I and alkene, and diiodoalkanes), has not found favor. We became interested in exploring the assumed mechanism more rigorously during our recent study of an iodine-catalyzed isomerization of a phenyl-pentenone.¹⁶ The goals of this research project were (i) to use accurate quantum chemistry computations to evaluate the assumed three-step mechanism and (ii) to use the results to examine the differences in molecular pathways and energetics among several different alkenes.

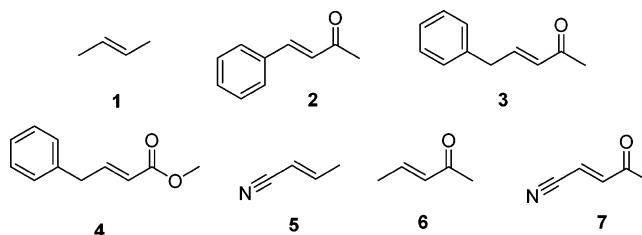


Figure 1. The seven 1,2-disubstituted alkenes investigated.

This study investigates the catalyzed *cis/trans* isomerizations of 2-butene and six 1,2-disubstituted alkenes, 1–7 (Figure 1). We will discuss, in order, (i) conformer optimizations for the *cis* and *trans* isomers, (ii) the regiospecificity of I-atom addition, (iii) connected three-step pathways and energy profiles for all seven molecules, and (iv) single-point energies at higher levels of theory for improved accuracy.

Theoretical Methods

Most calculations were performed with the software package Gaussian 98,¹⁷ but the coupled-cluster single-point calculations for the isomerization paths were performed with MOLPRO 2002.¹⁸

Geometry optimizations were performed with three computational methods: semiempirical AM1,¹⁹ ab initio Hartree–Fock (HF), and density functional (B3LYP)^{20,21} theory. Radical species were studied with both unrestricted (U) and restricted (RO) open-shell calculations, but RO results were preferred because of poor spin-density results with unrestricted calculations (possibly due to bad spin contamination). Because the Gaussian 98 eigenvector-following (EF) algorithm²² limits transition-state geometry optimizations to 50 variables or less, calculations on **2** (60 variables including the I atom) had variables within the phenyl ring held constant, and calculations on **3** and **4** had phenyl and methyl variables held constant.

Molecular energies were computed with these methods as well as with Møller–Plesset second-order perturbation theory (MP2),²³ the spin-projected variants of HF and MP2,²⁴ and the coupled-cluster²⁵ approximations RHF–RCCSD(T) and

* To whom correspondence should be addressed. E-mail: allan.east@uregina.ca.

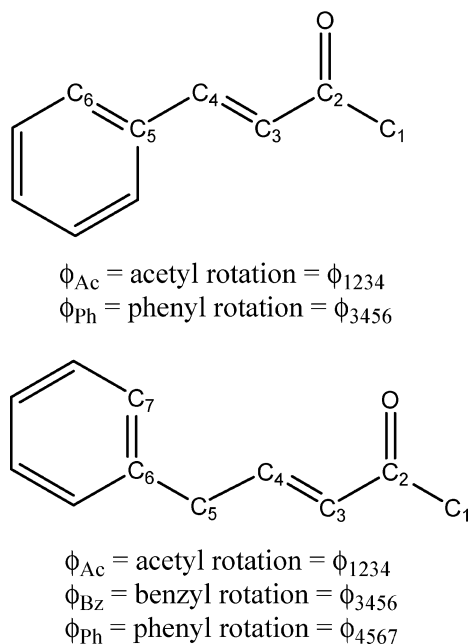


Figure 2. Our dihedral angle conventions for molecules **2** (top) and **3** (bottom).

RHF–UCCSD(T),^{26,27} which we denote RRCCSD(T) and RUCCSD(T), respectively. All corrections for free energy and enthalpy values were computed from ROHF with the mixed basis set (see below), using standard statistical thermodynamics formulas at 298 K and 1 atm. All energy profile figures consider the cis isomer as the reactant on the extreme left and the trans isomer as the product on the extreme right, with molecular energies expressed relative to that of the trans product.

The basis set generally used was Dunning’s cc-pVDZ basis set;²⁸ however, this basis set is not defined for iodine atoms. Hence, our “mixed” basis set uses cc-pVDZ for all non-I atoms and the Los Alamos LANL2DZ basis set²⁹ for I. The LANL2DZ set contains effective core potentials (ECPs) for large atoms, to reduce the number of electrons involved in the calculations. In the case of iodine, the ECP covers all except the two 5s and five 5p electrons. The biggest deficiency in the LANL2DZ basis set is that it lacks polarization functions (i.e., d functions) for

valence electrons. In our benchmark calculations, we used the prescriptions of Radom and co-workers³⁰ for improving upon the LANL2DZ iodine basis set: the polarization functions used were the ones appropriate for the Hay–Wadt ECP for energy (rather than optimization) calculations, and for TZ(2d,f), we uncontracted the LANL2DZ valence functions as Radom and co-workers did.

Results and Discussion

Conformational Searches. Because many of the chosen molecules have multiple conformations, we began with a detailed conformational search for the two phenylalkenones **2** and **3**. Figure 2 shows our labeling conventions for the two molecules.

The initial AM1 search involved optimizations from 150 starting geometries (25 *cis*-**2**, 25 *trans*-**2**, 50 *cis*-**3**, 50 *trans*-**3**), but the results were of little worth because they disagreed badly with ensuing HF/cc-pVDZ and B3LYP/cc-pVDZ optimizations. The failure of AM1 here is likely due to the absence of phenyl groups in the set of molecules used for AM1’s parametrization in the early 1980s. The HF and B3LYP optimizations of **2** and **3** were generally in very good agreement, and the following general rules were learned: (i) methyl groups adjacent to a C=O group prefer a C–H bond eclipsed to the C=O bond, (ii) acetyl groups adjacent to a C=C group can take on $\phi_{Ac} = 0^\circ$ or 180° , but prefer the C=O bond to be eclipsed to the C=C bond ($\phi_{Ac} = 180^\circ$), (iii) phenyl groups adjacent to a –CH₂R group prefer a “pan-handle” geometry ($\phi_{Ph} = 90^\circ \pm 30^\circ$), (iv) phenyl groups adjacent to a C=C group prefer a planar geometry ($\phi_{Ph} = 0^\circ$), and (v) benzyl groups adjacent to a C=C group can take on $\phi_{Bz} = 0^\circ$ or $\pm 120^\circ$.

These general rules were applied to the remaining molecules **1** and **4–7**, simplifying their conformational searches. Table 1 lists the B3LYP/cc-pVDZ results for all of the conformers found in this study. Note from Table 1 that the actual values of the dihedral angles can vary substantially from the idealized general-rule values, particularly in the case of the cis structures, where steric hindrance plays a significant role.

Iodo Intermediates. The search for β -iodo intermediates was done at the ROHF/mixed level, because of difficulties with B3LYP optimizations (see the end of this section). Adding an

TABLE 1: Summary of B3LYP/cc-pVDZ-Optimized Cis and Trans Isomers

molecule	isomer	conformer-defining dihedral angles ^a	<i>E</i> (kJ mol ^{−1}) ^b
2-butene (1)	trans	none	0.00
	cis	none	5.35
4-phenylbut-3-en-2-one (2)	trans 1	$\phi_{Ph} = 0^\circ, \phi_{Ac} = 180^\circ$	0.00
	trans 2	$\phi_{Ph} = 0^\circ, \phi_{Ac} = 0^\circ$	4.06
	cis 1	$\phi_{Ph} = 0^\circ, \phi_{Ac} = 180^\circ$	16.90
	cis 2	$\phi_{Ph} = -149^\circ, \phi_{Ac} = 50^\circ$	35.47
5-phenylpent-3-en-2-one (3)	trans 1	$\phi_{Ph} = -90^\circ, \phi_{Bz} = 0^\circ, \phi_{Ac} = 180^\circ$	0.00
	trans 2	$\phi_{Ph} = -90^\circ, \phi_{Bz} = 0^\circ, \phi_{Ac} = 0^\circ$	4.75
	trans 3	$\phi_{Ph} = -66^\circ, \phi_{Bz} = 123^\circ, \phi_{Ac} = 180^\circ$	0.18
	trans 4	$\phi_{Ph} = -68^\circ, \phi_{Bz} = 123^\circ, \phi_{Ac} = 0^\circ$	2.09
	cis 1	$\phi_{Ph} = -82^\circ, \phi_{Bz} = 107^\circ, \phi_{Ac} = 167^\circ$	4.24
	cis 2	$\phi_{Ph} = -62^\circ, \phi_{Bz} = 127^\circ, \phi_{Ac} = 1^\circ$	21.13
methyl 4-phenylbut-3-enoate (4)	trans	$\phi_{Ph} = -90^\circ, \phi_{Bz} = 0^\circ, \phi_{Ac} = 180^\circ$	0.00
	cis	$\phi_{Ph} = -83^\circ, \phi_{Bz} = 108^\circ, \phi_{Ac} = 179^\circ$	2.56
2-butenitrile (5)	trans	none	0.00
	cis	none	−0.60
3-penten-2-one (6)	trans	$\phi_{Ac} = 180^\circ$	0.00
	cis	$\phi_{Ac} = 180^\circ$	7.38
4-oxo-2-pentenitrile (7)	trans	$\phi_{Ac} = 180^\circ$	0.00
	cis	$\phi_{Ac} = 180^\circ$	13.23

^a Dihedral angles are defined in Figure 2. ^b Energies are expressed relative to the lowest-energy trans isomer of each molecule.

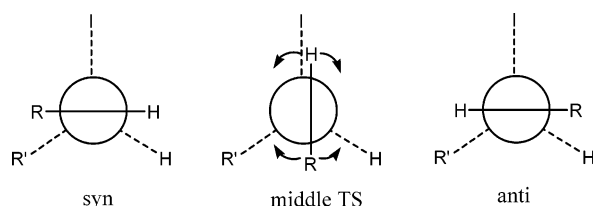


Figure 3. Syn intermediate, middle transition state, and anti intermediate for iodine-catalyzed equilibration of 1,2-disubstituted alkenes, according to ROHF/mixed level of theory. Note that the preferred middle TS involved eclipsing H with I, rather than R with I, in all seven molecules studied here.

TABLE 2: Regiospecific Effects: Relative Energies of Alternative Syn Iodo Intermediates, upon Addition of I Atom to the C=C Unit of Asymmetric Cis-Substituted Alkenes

HCR'=RCH	R	R'	E_{diff} (kJ mol ⁻¹) ^a
4-phenylbut-3-en-2-one (2)	Ac	Ph	3
5-phenylpent-3-en-2-one (3)	Bz	Ac	34
methyl-4-phenylbut-3-enoate (4)	Bz	COOMe	23
2-butenenitrile (5)	Me	CN	26
3-penten-2-one (6)	Me	Ac	21
4-oxo-2-pentenitrile (7)	Ac	CN	5

^a $E(\text{HCR}-\text{CHR}'\text{I}) - E(\text{HCRI}-\text{CHR}')$, i.e., the energetic benefit of adding iodine to the carbon nearest R vs the carbon nearest R', computed with ROHF/mixed.

I atom to $\text{RHC}=\text{CHR}$ converts an sp^2 carbon atom to an sp^3 chiral carbon center, conceivably resulting in as many as six staggered C_1 -symmetry conformers with $\phi_{\text{R}'\text{CCR}}$ values of $\pm 30^\circ$, $\pm 90^\circ$, and $\pm 150^\circ$. The preference for staggered structures over eclipsed ones (0° , $\pm 60^\circ$, $\pm 120^\circ$, 180°) is due to a hyperconjugation benefit for the radical carbon p orbital to be eclipsed to a $\sigma_{\text{C}-\text{X}}$ bond. We tested all six staggered conformer possibilities for the addition of I to 2-butene, but only two minima were found (Figure 3): a syn intermediate ($\phi_{\text{CCCC}} = 38^\circ$) and an anti intermediate ($\phi_{\text{CCCC}} = -163^\circ$). This preference could be due to the steric influence of the I atom, although the hyperconjugative benefit is maximized when the radical carbon p orbital eclipses a $\sigma_{\text{C}-\text{I}}$ bond in particular.³¹ Hence, for all ensuing molecules, only these two intermediate conformers were probed, and such intermediates existed in all cases at this level of theory.

We investigated the regiospecificity for iodine attachment to the six asymmetric *cis*-1,2-disubstituted alkenes. Table 2 lists the magnitudes of energetic benefit for adding an I atom to the carbon attached to R vs the carbon attached to R' for each molecule, creating syn intermediates. For molecules 3–6, the alkene double bond was conjugated only on one side, and the clear preference (> 20 kJ mol⁻¹) is for iodine attachment to the unconjugated side to allow for resonance stabilization of the resulting radical. For the other two molecules, the C=C bond is originally conjugated on both sides; the weak preference here is for the created radical to resonate with phenyl or cyano groups rather than the acetyl group.

TABLE 3: Summary of $\phi_{\text{CC}=\text{CC}}$ Dihedral Angles from ROHF/Mixed Level of Theory

molecule	cis						trans
	product + I•	syn TS	syn INT	mid TS	anti INT	anti TS	product + I•
2-butene (1)	0°	25°	39°	-72°	-163°	-166°	-180°
4-phenylbut-3-en-2-one (2)	0°	38°	59°	-7°	-158°	-163°	-180°
5-phenylpent-3-en-2-one (3)	0°	21°	40°	-27°	-143°	-161°	-180°
methyl 4-phenylbut-2-enoate (4)	0°	21°	41°	-27°	-144°	-160°	-180°
2-butenenitrile (5)	0°	18°	31°	-59°	-150°	-161°	-180°
3-penten-2-one (6)	0°	18°	34°	-36°	-143°	-160°	-180°
4-oxo-2-pentenitrile (7)	0°	21°	47°	-19°	-156°	-164°	-180°

Isomerization Paths. Transition states for the iodine-association and *cis/trans*-isomerization steps were next found for all molecules. The iodine-association transition states were unambiguous. The “middle” step, *syn/anti* isomerization, has a choice of two paths with different barrier heights, because once the iodine atom anchors one side of the former C=C double bond, the other side can rotate clockwise or counterclockwise, to eclipse the created $\sigma_{\text{C}-\text{I}}$ bond with either a $\sigma_{\text{C}-\text{R}}$ or $\sigma_{\text{C}-\text{H}}$ bond. For all seven molecules, the preferred direction has the alkyl arm swinging away from the iodine, to avoid having to eclipse the large atom.

Table 3 lists the $\phi_{\text{CC}=\text{CC}}$ dihedral angles for the isomerization paths of all seven molecules. Note that the minimum-energy path does not feature a monotonic decrease of $\phi_{\text{CC}=\text{CC}}$ from 0° to -180° , but first features an increase to over $+30^\circ$ (syn intermediate) before changing direction. The location of the middle transition state varies widely among the molecules, with $\phi_{\text{CC}=\text{CC}}$ values between -7° and -72° .

The optimized C–I bond distances were fairly consistent across the seven-molecule set, being 2.53 ± 0.05 Å in the association transition states, 2.27 ± 0.04 Å in the intermediates, and 2.22 ± 0.04 Å in the middle transition state. The intermediates have slightly longer C–I bonds than the middle transition state because the C–I bond order is slightly less than 1, as demonstrated in Figure 4: hyperconjugation is more prevalent in the intermediates than in the transition state, and according to the resonance-theory formulation of hyperconjugation, the intermediates see a 7–11% contribution (see spin-density results below) from a Lewis resonance structure with an iodine radical and a C–I bond order of 0.

We tried to improve the level of theory to ROB3LYP for geometry optimizations, but five of the first six optimizations we tried for intermediates simply resulted in dissociation of the iodine atom. Hence, the ROB3LYP and ROHF calculations disagree on the existence of intermediates in iodine-catalyzed *cis/trans* isomerization. This issue was examined with higher levels of theory (see Energetics section below).

Odd-Electron Spin Densities. Tables 4 and 5 list the total-electron ROHF/mixed Mulliken-population spin densities assigned to, respectively, the iodine atom and the “radical carbon” atom (the C atom in the C=C double bond that bears the most radical character when the I atom attaches to the other carbon). Table 4 shows that, as the iodine atom attaches to the alkene, it transfers most of its radical character, leaving 7–11% on I in the intermediates and 0–6% on I in the middle transition state. Table 5 shows that most of the transferred radical character appears on the radical carbon, up to 72–85% in the intermediates and 81–93% in the middle transition state. By this measure, the degree of hyperconjugation of the minor electronic structure in Figure 4 is 5% greater in the intermediates than in the middle transition state.

In comparing molecules, we can see varying levels of radical resonance stabilization. Consider the anti intermediate column in Table 5: the lowest value (0.72) for the spin density on the

TABLE 4: Summary of ROHF/Mixed Electron Spin Density Localized on the Iodine Atom

molecule	cis product + I•	syn TS	syn INT	mid TS	anti INT	anti TS	trans product + I•
2-butene (1)	1.00	0.30	0.10	0.00	0.10	0.30	1.00
4-phenylbut-3-en-2-one (2)	1.00	0.31	0.09	0.06	0.11	0.29	1.00
5-phenylpent-3-en-2-one (3)	1.00	0.38	0.07	0.02	0.07	0.37	1.00
methyl 4-phenylbut-2-enoate (4)	1.00	0.38	0.07	0.00	0.07	0.39	1.00
2-butenitrile (5)	1.00	0.39	0.08	0.00	0.07	0.40	1.00
3-penten-2-one (6)	1.00	0.38	0.08	0.01	0.07	0.39	1.00
4-oxo-2-pentenenitrile (7)	1.00	0.42	0.07	0.03	0.07	0.42	1.00

TABLE 5: Summary of ROHF/Mixed Electron Spin Density Localized on the Radical Carbon

molecule	cis product + I•	syn TS	syn INT	mid TS	anti INT	anti TS	trans product + I•
2-butene (1)	0.00	0.60	0.85	0.93	0.84	0.60	0.00
4-phenylbut-3-en-2-one (2)	0.00	0.50	0.75	0.81	0.72	0.52	0.00
5-phenylpent-3-en-2-one (3)	0.00	0.52	0.82	0.85	0.82	0.53	0.00
methyl 4-phenylbut-2-enoate (4)	0.00	0.52	0.83	0.88	0.83	0.52	0.00
2-butenitrile (5)	0.00	0.50	0.82	0.87	0.82	0.50	0.00
3-penten-2-one (6)	0.00	0.52	0.82	0.86	0.82	0.51	0.00
4-oxo-2-pentenenitrile (7)	0.00	0.48	0.83	0.84	0.82	0.48	0.00

radical carbon occurred when the radical carbon was attached to a phenyl ring, allowing a great deal of radical resonance. The next lowest value (0.82) occurred in the four cases when the radical was stabilized by a cyano or acetyl group. The highest value (0.84) occurred when the radical carbon was attached to a methyl group, which provides only hyperconjugative resonance stability.

Energetics. More accurate energies were desired to address two issues: (i) the existence of intermediates and (ii) the variations among several alkenes. Single-point calculations were performed at ROHF/mixed geometries, because of the absence

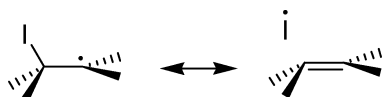


Figure 4. Major (left) and minor (right) resonance structures for iodo intermediates, to explain hyperconjugative reduction of the C–I bond order. The minor structure contributes even less at the internal-rotation (middle) transition state.

of intermediates with ROB3LYP. Fortunately, the effect of the ROHF geometry approximation on relative ΔE values is diminished by cancellation of errors (i.e., bond lengths are uniformly underpredicted) and is likely to be smaller than the energy approximations made by the various levels of theory.

Figures 5–7 show plots of the results of many electronic structure methods (with the mixed LANL2DZ/cc-pVDZ basis set) for the electronic energies (without ZPVE, temperature, or spin–orbit corrections) of the iodine-catalyzed cis/trans equilibration of the first three alkenes. The wide range of predictions is alarming, with some levels of theory evidently in error both qualitatively and quantitatively. Note in particular that several levels of theory *do not* predict the existence of intermediates, disagreeing with ROHF/mixed (black X's with solid line) and with the conventional mechanism championed by Benson.

To further evaluate these methods, we turned to two benchmark calculations from the literature: the C–I dissociation reaction $C_2H_5I \rightarrow C_2H_5 + I$ and the HI proton affinity reaction

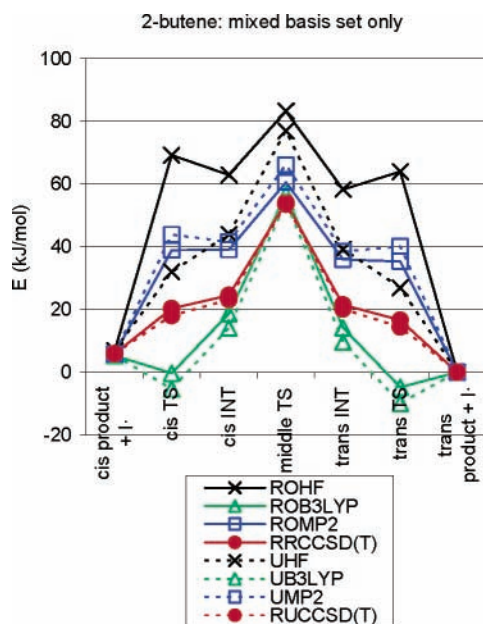


Figure 5. Isomerization energy profiles (cis \rightarrow trans) for 2-butene, at different levels of theory using ROHF/mixed geometries.

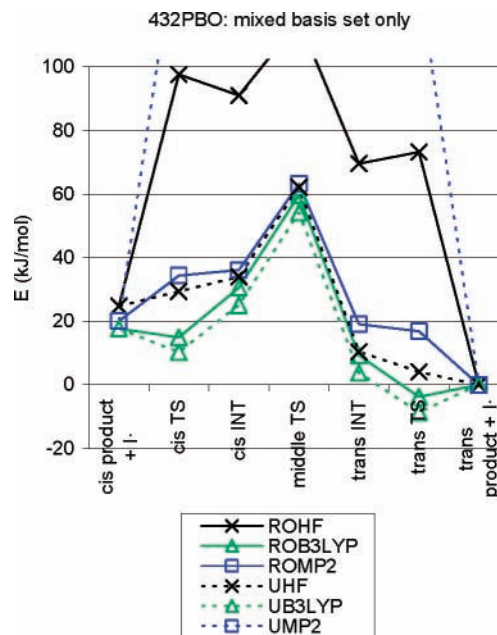


Figure 6. Isomerization energy profiles (cis \rightarrow trans) for alkene 2, at different levels of theory using ROHF/mixed geometries.

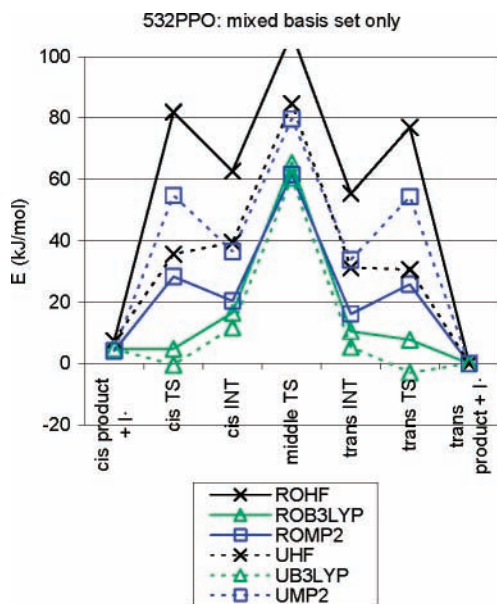


Figure 7. Isomerization energy profiles (cis \rightarrow trans) for alkene **3**, at different levels of theory using ROHF/mixed geometries.

TABLE 6: Computed 298 K Enthalpies for $C_2H_5I \rightarrow C_2H_5 + I$ ($kJ\ mol^{-1}$)^a

	ROB3LYP	ROMP2	UMP2	PUMP2	RUCCSD(T)
DZ ^b	194	188	188	183	189
DZ(d) ^c		211	213	205	199
DZ(df) ^d	214	225	228	218	211
TZ(2df) ^e		234	238	227	219
NIST data ^a					233
expt ^a					222

^a Gaussian 98 calculations. Single-point calculations at ROB3LYP/mixed-optimized geometries. Table values include thermal corrections from ROHF/mixed frequencies and a $-30\ kJ\ mol^{-1}$ spin-orbit correction for I atom from ref 32. NIST data, ref 33; expt data, ref 34. ^b DZ: LANL2DZ for I, cc-pVDZ for C/H. ^c DZ(d): LANL2DZ plus *1d* for I, cc-pVDZ for C/H. ^d DZ(df): LANL2DZ plus *1d1f* for I, cc-pVDZ for C/H. ^e TZ(2df): uncontracted LANL2DZ plus *2d1f* for I, cc-pVTZ for C/H.

TABLE 7: Computed 298 K Enthalpies for $H_2I^+ \rightarrow HI + H^+$ ($kJ\ mol^{-1}$)^a

	B3LYP	MP2	CCSD(T)
DZ	609	635	653
DZ(d)		623	642
DZ(df)	623	619	633
TZ(2df)		622	632
Lias data ^a			615
expt ^a			618(10)

^a Gaussian 98 calculations. Single-point calculations at B3LYP/mixed optimized geometries. Table values include thermal corrections from ROHF/mixed frequencies. See Table 6 for basis set descriptions. Lias data: ref 35. Expt. data: ref 36.

$H_2I^+ \rightarrow HI + H^+$. Tables 6 and 7, respectively, report our computed results for these two reactions. These results suggest that polarization functions on the I atom are essential for good energetics and that CCSD(T)/TZ(2df) is (as usual) a very good target level of achievement.

Figure 8 presents a plot of the reaction energy profile for 2-butene (still without ZPVE, temperature, or spin-orbit corrections), showing the effects of varying the basis set. We note two important features. First, the addition of polarization functions onto the hydrocarbon atoms (going from blue X's to blue stars) shifts the curve slightly, but adding polarization functions onto the I atom (going from stars to diamonds with

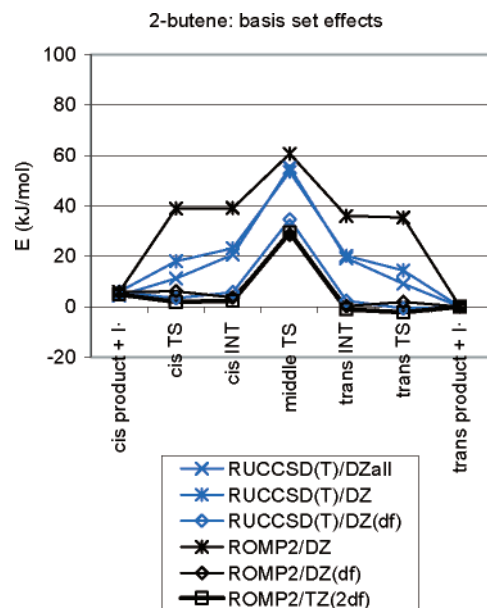


Figure 8. Isomerization energy profile (cis \rightarrow trans) for 2-butene, using different basis sets. Basis sets are as described in Table 6, except for DZall, which used LANL2DZ on every atom.

either color) shifts the curve significantly. Second, the small energy shifts in going from ROMP2/DZ(df) to RUCCSD(T)/DZ(df) (black diamonds to blue diamonds) suggests that the ideal curve (for RUCCSD(T)/TZ(2df), which was too large a calculation for our computer) should be close to the ROMP2/TZ(2df) curve. Hence, ROMP2/TZ(2df) single-point calculations were performed for all seven reactions to provide our most accurate final energetics; they are predicted to be within $5\ kJ\ mol^{-1}$ of CCSD(T) values and $20\ kJ\ mol^{-1}$ of the true values.

Table 8 presents our best predictions for the enthalpies of the seven reactions. Trans isomers seem to have slightly more affinity than cis ones for iodine atoms, but none of them are bound by more than $7\ kJ\ mol^{-1}$ relative to iodine dissociation. Of these seven alkenes, the one with the most stable iodo intermediates is 5-phenylpent-3-en-2-one (**3**).

More interestingly, these data predict iodo intermediates for alkenes **3–7**, but not **1** or **2**. This is likely because **1** and **2** would have *significant interruption of π bonding or π -type conjugation* in their iodo intermediates. The intermediate for **1** (2-butene) is not stable because iodo attachment reduces the number of π -type electrons from two bonding electrons to one nonbonding electron. The intermediate for **2** is not stable because the initial conjugation of 10 π electrons would be broken up into a resonant set of 7 on one side and a carbonyl pair on the other. The only other case where significant conjugative interruption would occur is for **7**, where six conjugated π electrons are split into a set of three and a carbonyl pair, and the iodo intermediate, at least for the cis form, is only barely stable. The other four molecules involve a milder reduction in conjugation, from six π electrons to five or from four to three, which are less severe and still allow stabilization of the radical and, hence, allow for weakly stable intermediates.

The rate-determining step in all seven reactions is the middle step, as deduced by Benson many years ago. The variation in overall barrier heights, relative to the dissociated trans products (set at the energy zero), is from 35 to $59\ kJ\ mol^{-1}$. The most significant effect is the extra steric hindrance in the internal-rotation transition state for compounds **2–4** relative to compounds **5–7**.

TABLE 8: Best Computed 298 K Relative Enthalpies for Cis \rightarrow Trans Isomerization of Alkenes (kJ mol⁻¹)^a

molecule	cis product + I•	syn TS	syn INT	mid TS	anti INT	anti TS	trans product + I•
2-butene (1)	5.53	28.03	31.21	54.54	27.36	23.35	0.00
4-phenylbut-3-en-2-one (2)	22.26	23.44	28.21	51.98	8.69	2.87	0.00
5-phenylpent-3-en-2-one (3)	7.26	21.87	16.51	48.65	11.01	17.80	0.00
methyl 4-phenylbut-2-enoate (4)	5.97	24.81	22.59	59.31	18.97	21.81	0.00
2-butenitrile (5)	-1.89	23.62	21.47	35.42	22.66	26.04	0.00
3-penten-2-one (6)	9.20	29.64	27.22	38.58	17.11	21.40	0.00
4-oxo-2-pentenitrile (7)	12.39	34.97	34.17	39.12	19.47	23.21	0.00

^a Single-point RMP2/TZ(2df) Gaussian 03 calculations at ROHF/mixed-optimized geometries. Table values include ZPVE and thermal corrections from ROHF/mixed frequencies and a -30 kJ mol⁻¹ spin-orbit correction for I atom (columns 2 and 8) from ref 32. See Table 6 for the TZ(2df) basis set description.

A final comment is warranted for the case of 2-butene in particular. Our calculations predict an intermediate-free one-step mechanism for I-atom catalysis. However, Benson and co-workers,⁷ as well as Back and Cvetanovic,⁸ successfully fitted kinetic analyses to model mechanisms involving intermediates. We offer three possible explanations for the discrepancy. First, the limitations in accuracy of our best approximations might have prevented us from detecting the assumed intermediates in the case of 2-butene. Second, the experimental data might be acceptably fit to a one-step mechanism. Third, if a two-step mechanism is truly needed, the intermediates might instead be π complexes as imagined by Back and Cvetanovic. We did a quick calculation of π -complex stability, but ROHF and RMP2 results greatly disagreed, and we were unsure of how much spin-orbit energy lowering to add to such complexes. Future work is recommended to evaluate the π -complex hypothesis in light of our current results.

Conclusions

The commonly assumed three-step mechanism for iodine-atom-catalyzed cis/trans isomerization of alkenes has been investigated by ab initio quantum chemical calculations. The calculations suggest that C-I bond strengths in the radical intermediates are extremely weak, when they exist at all; the predicted barriers to dissociation are 7 kJ mol⁻¹ or less, which is less than the likely accuracy of the calculations, so we cannot make strong conclusions on the existence of iodo intermediates. The reaction paths are not trivial, for the I atom can bond to either of the C=C carbons, and in each of our seven molecular cases the actual isomerization step proceeds with the "non-anchored arm" twisting away from the I atom, to avoid eclipsing it.

The phenomenon of radical resonance stabilization was observed, and trends are as anticipated. Once the iodine atom is covalently bonded, the bulk of the spin density is transferred to the carbon β to it. Furthermore, the lowest value (0.72) for the spin density on this radical carbon occurs when the radical carbon is attached to a phenyl ring, allowing a great deal of radical resonance. The next lowest value (0.82) occurs when the radical is stabilized by a cyano or acetyl group, and the highest value (0.84) occurs when the radical carbon is attached to a methyl group. Hyperconjugative effects explain why the middle transition state (internal rotation) has shorter C-I bond lengths and less radical character than the iodo intermediates.

Five of the seven alkenes are predicted to have fleetingly stable "hanging-well" intermediates, i.e., intermediates that are endothermic relative to reactants and yet only partway up a potential barrier. Their barriers relative to iodine-atom dissociation are <7 kJ mol⁻¹. A rough criterion for gauging whether an alkene will have stable iodo intermediates would be the

amount of π -type bonding or conjugation interruption by an iodo attachment. The two alkenes in our study that appear not to have intermediates, 2-butene and 4-phenylbut-3-ene-2-one, have stable π systems that are either eliminated or significantly reduced by hypothetical iodo attachment.

Acknowledgment. A. G. H. Wee is thanked for proposing the study and for valuable discussions. NSERC and CFI are thanked for funding. The Laboratory of Computational Discovery (University of Regina) is also thanked for use of its resources.

References and Notes

- Dickinson, R. G.; Lotzkar, H. *J. Am. Chem. Soc.* **1937**, *59*, 472.
- Golden, D. M.; Benson, S. W. *Chem. Rev.* **1969**, *69*, 125.
- Benson, S. W.; Bose, A. N. *J. Am. Chem. Soc.* **1963**, *85*, 1385.
- Benson, S. W.; Bose, A. N.; Nangia, P. *J. Am. Chem. Soc.* **1963**, *85*, 1388.
- Golden, D. M.; Egger, K. W.; Benson, S. W. *J. Am. Chem. Soc.* **1964**, *86*, 5416.
- Egger, K. W.; Golden, D. M.; Benson, S. W. *J. Am. Chem. Soc.* **1964**, *86*, 5420.
- Benson, S. W.; Egger, K. W.; Golden, D. M. *J. Am. Chem. Soc.* **1965**, *87*, 468.
- Back, M. H.; Cvetanovic, R. J. *Can. J. Chem.* **1963**, *41*, 1396.
- Back, M. H.; Cvetanovic, R. J. *Can. J. Chem.* **1963**, *41*, 1406.
- Carr, M. D.; Kane, V. V.; Whiting, M. C. *Proc. R. Chem. Soc.* **1964**, 408.
- Maryanoff, B. E.; Reitz, A. B. *Chem. Rev.* **1989**, *89*, 863.
- Vedejs, E.; Peterson, M. J. *Top. Stereochem.* **1994**, *21*, 1.
- Saltiel, J.; Ganapathy, S.; Werking, C. *J. Phys. Chem.* **1987**, *91*, 2755.
- Muizebelt, W. J.; Nivard, R. J. F. *J. Chem. Soc. B* **1968**, 913.
- Gaukroger, K.; Hadfield, J. A.; Hepworth, L. A.; Lawrence, N. J.; McGown, A. T. *J. Org. Chem.* **2001**, *66*, 8135.
- East, A. L. L.; Wang, Z.; Wee, A. G. H.; Hepperle, S. S.; Treble, R. G. Manuscript in preparation.
- Frisch M. J.; Trucks G. W.; Schlegel H. B.; Scuseria G. E.; Robb M. A.; Cheeseman J. R.; Zakrzewski V. G.; Montgomery J. A., Jr.; Stratmann R. E.; Burant J. C.; Dapprich S.; Millam J. M.; Daniels A. D.; Kudin K. N.; Strain M. C.; Farkas O.; Tomasi J.; Barone V.; Cossi M.; Cammi R.; Mennucci B.; Pomelli C.; Adamo C.; Clifford S.; Ochterski J.; Petersson G. A.; Ayala P. Y.; Cui Q.; Morokuma K.; Malick D. K.; Rabuck A. D.; Raghavachari K.; Foresman J. B.; Cioslowski J.; Ortiz J. V.; Baboul A. G.; Stefanov B. B.; Liu G.; Liashenko A.; Piskorz P.; Komaromi I.; Gomperts R.; Martin R. L.; Fox D. J.; Keith T.; Al-Laham M. A.; Peng C. Y.; Nanayakkara A.; Challacombe M.; Gill P. M. W.; Johnson B.; Chen W.; Wong M. W.; Andres J. L.; Gonzalez C.; Head-Gordon M.; Replogle E. S.; Pople J. A. *Gaussian 98*, revision A.9; Pittsburgh, PA, 1998.
- Werner, H.-J.; Knowles, P. J.; Schütz, M.; Lindh, R.; Celani, P.; Korona, T.; Rauhut, G.; Manby, F. R.; Amos, R. D.; Bernhardsson, A.; Berning, A.; Cooper, D. L.; Deegan, M. J. O.; Dobbyn, A. J.; Eckert, F.; Hampel, C.; Hetzer, G.; Lloyd, A. W.; McNicholas, S. J.; Meyer, W.; Mura, M. E.; Nicklass, A.; Palmieri, P.; Pitzer, R.; Schumann, U.; Stoll, H.; Stone, A. J.; Tarroni, R.; Thorsteinsson, T. *MOLPRO 2002.6*; University of Birmingham, Birmingham, U.K., 2002.
- Dewar, M. J. S.; Zoebisch, E. G.; Healy, E. F.; Stewart, J. J. P. *J. Am. Chem. Soc.* **1985**, *107*, 3902.
- Becke, A. D. *J. Chem. Phys.* **1993**, *98*, 5648.
- Lee, C.; Yang, W.; Parr, R. G. *Phys. Rev. B* **1988**, *37*, 785.

- (22) Baker, J. J. *Comput. Chem.* **1986**, 7, 385.
(23) Møller, C.; Plesset, M. S. *Phys. Rev.* **1934**, 46, 618.
(24) Schlegel, H. B. *J. Chem. Phys.* **1986**, 84, 4530.
(25) Bartlett, R. J. *J. Phys. Chem.* **1989**, 93, 1697.
(26) Knowles, P. J.; Hampel, C.; Werner, H.-J. *J. Chem. Phys.* **1993**, 99, 5219.
(27) Knowles, P. J.; Hampel, C.; Werner, H.-J. *J. Chem. Phys.* **2000**, 112, 3106.
(28) Dunning, T. H., Jr. *J. Chem. Phys.* **1989**, 90, 1007.
(29) Wadt, W. R.; Hay, P. J. *J. Chem. Phys.* **1985**, 82, 284.
(30) Glukhovtsev, M. N.; Pross, A.; McGrath, M. P.; Radom, L. *J. Chem. Phys.* **1995**, 103, 1878.
(31) The σ_{C-I} bond is particularly sensitive to hyperconjugative effects because the C–I bond is weak; the poor orbital overlap results in a small $\sigma-\sigma^*$ energy gap, with a penchant for biradical character. Hence, the presence of a radical electron on a neighboring carbon atom, aligned to overlap as best it can with the C–I bond, is strongly energetically favored.

- This small $\sigma-\sigma^*$ gap, and a discussion of hyperconjugative effects in substituted ethanes, can be seen in the data and discussion of Alabugin, I. V.; Zeidan, T. A. *J. Am. Chem. Soc.* **2002**, 124, 3175.
(32) Stevens, J. E.; Cui, Q.; Morokuma, K. *J. Chem. Phys.* **1998**, 108, 1544.
(33) Afeefy, H. Y.; Liebman, J. F.; Stein, S. E. Neutral Thermochemical Data. In *NIST Chemistry WebBook*; NIST Standard Reference Database Number 69; Mallard, W. G., Linstrom, P. J., Eds.; National Institute of Standards and Technology: Gaithersburg, MD, June 2005 (<http://webbook.nist.gov>).
(34) Rosenstock, H. M.; Draxl, K.; Steiner, B. W.; Herron, J. T. *J. Phys. Chem. Ref. Data* **1977**, 6 (Suppl. 1).
(35) Lias, S. G.; Bartmess, J. E.; Liebman, J. F.; Holmes, J. L.; Levin, J. L.; Mallard, W. G. *J. Phys. Chem. Ref. Data* **1988**, 17 (Suppl. 1).
(36) McMahon, T. B. University of Waterloo, private communication, 2005.